On-surface homocoupling reactivity of a chiral bifunctional bromoindanone molecule on Cu(111)

Fatima Hussein, Corentin Pigot, Francisco Romero Lairado, Marco Minissale, Eric Salomon, Thierry Angot, Frédéric Dumur, Malek Nechab, Didier Gigmes, Sylvain Clair, et al.

On-surface homocoupling reactivity of a chiral bifunctional bromoindanone molecule on Cu(111)

Fatima Hussein [a], Corentin Pigot [c], Francisco Romero Lairado [b], Marco Minissale [b], Eric Salomon [b], Thierry Angot [b], Frédéric Dumur [c], Malek Nechab [c], Didier Gigmes [c], Sylvain Clair [a],*, Luca Giovanelli [a],*

[a] Aix-Marseille Univ, CNRS, IM2NP, Marseille, France.

[b] Aix-Marseille Univ, CNRS, PIIM, Marseille France.

[c] Aix-Marseille Univ, CNRS, ICR, UMR 7273, F-13397 Marseille, France.

* Corresponding authors: luca.giovanelli@im2np.fr; sylvain.clair@cnrs.fr

Abstract

On-surface synthesis has provided exciting concepts for the building of covalently bonded molecular nanostructures as well as the exploration of new synthetic pathway alternatives to chemical synthesis in solution. The surface-supported reaction of precursor molecules can result in the formation of 2D molecular networks as well as novel 0D molecular structures. In this study, we investigate in ultrahigh vacuum by low-temperature scanning tunneling microscopy the adsorption of the chiral molecule (*R*)-6-bromo-3-phenyl-2,3-dihydro-1*H*-inden-1-one (BrPhINDO) on the Cu(111) surface. Annealing an as-deposited layer of molecules allows to activate two kinds of homocoupling reactions, the Ullmann-like coupling and the Knoevenagel reaction, resulting in the formation of various low-dimensional structures. By studying their prochirality and comparing with the products obtained with the enantiomer precursor, we demonstrate adsorption-induced chiral inversion inducing partial racemization.

Introduction

One of the goals of nanotechnology is the construction of functional devices based on robust covalently bonded nanoarchitectures with atomic precision obtained by the bottom-up organization of well-designed precursor molecules. On-surface chemistry is a recent research field with great potential for the bottom-up production of specific nanostructures.[1-8] Pioneering studies described, e.g., the formation of a covalent bond between two iodobenzene molecules,[9] the thermally activated synthesis of an oligomer of porphyrin,[10] or the formation of extended graphene nanoribbons.[11] While the latter strategy to growth one dimensional (1D) systems was rather successful, the growth of two-dimensional (2D) covalent structures is more challenging.[12-15] In this approach, the molecular building blocks are deposited on a well-defined metal surface in (sub)monolayer regime and the homocoupling reaction is activated by thermal annealing. Scanning tunneling microscopy (STM) in ultrahigh vacuum (UHV) conditions is a tool of choice for the study of the nanostructures resulting from on-surface synthesis, providing a resolution at the single molecule level. The metallic substrates used, such as copper, silver and gold single crystals, provide usually an important catalytic activity and take a fundamental role into the reaction mechanism. Over the years, several reaction mechanisms for the covalent coupling of molecular building blocks have been extensively studied, among them the Ullmann-,[10,11,16-18] the Glaser-[19-21] or the Knoevenagel-type[22-24] reactions.

In this context, the molecular building blocks based on indanone are interesting because they can form covalent networks upon high temperature annealing, as e.g. with *s*-indacene-1,3,5,7(*2H*,*6H*)-tetrone ($INDO_4$).[25,26] This latter molecule is a symmetrical precursor with several O and H peripheral atoms which make it a highly versatile structure in terms of self-assembly[27,28] and reactivity.[24,29] However, the repartition of the 4 O atoms in D_{2h} high symmetry allows a variety of different coupling configurations, which can be a source of disorder precluding the formation of extended 2D covalent networks.[24] In principle this can be circumvented simply by reducing the symmetry, as it is the case for indan-1,3-dione as compared to indan-1,3,5,7-tetrone.[21] On a surface, a further source of disorder for planar achiral molecules comes from the adsorption-induced prochiral asymmetry. Prochiral racemization upon adsorption can be avoided by using an intrinsically chiral precursor bearing a bulky group on its asymmetric carbon.[30,31] In fact, the issue of controlling the chirality of covalent products on a surface is actively pursued in recent years.[32,33] It was shown that chirality control can be achieved by depositing chiral and/or prochiral precursors and that it can even be transferred to co-deposited achiral molecules.[30,32,33] On the other hand, it has been shown that the introduction of a bifunctionality in the molecular precursor producing an adequate sequential reactivity can improve the growth process in on-surface polymerization.[4,12,34,35]

We have thus designed the molecular precursor (*R*)-6-bromo-3-phenyl-2,3-dihydro-1*H*-inden-1-one (BrPhINDO, Fig. 1) as a model system. It is composed of a 1-indanone backbone substituted with a bromine atom at the 6-position and a phenyl group at the 3-position. This chiral molecule is expected to adsorb with the indanone backbone preferentially on one side due to the strong interaction of the carbonyl group with the metal surface and the presence of the bulky phenyl group on the asymmetric carbon. Based on previous results reported in the literature for indacene-1,3,5,7-tetrone,[24,29] multiple reactivity leading to different intermolecular couplings can take place with these molecular tectons, leading to intermolecular couplings such as Knoevenagel or oxidative couplings. In the case of BrPhINDO, the concomitant presence of a bromine can be at the origin of numerous couplings (see Fig. 1), what is examined in this work.

The Cu(111) surface was chosen as reaction template due to its hexagonal symmetry and its high reactivity[36] with respect to other coinage metals, in particular towards halogenated precursors.[4,18,37] Also, the copper surface is expected to favor the flat adsorption of the precursor that has an intrinsically 3D structure. The formation of the different reaction products was studied by low-temperature scanning tunneling microscopy (LT-STM) in combination with core-level photoemission spectroscopy (XPS).

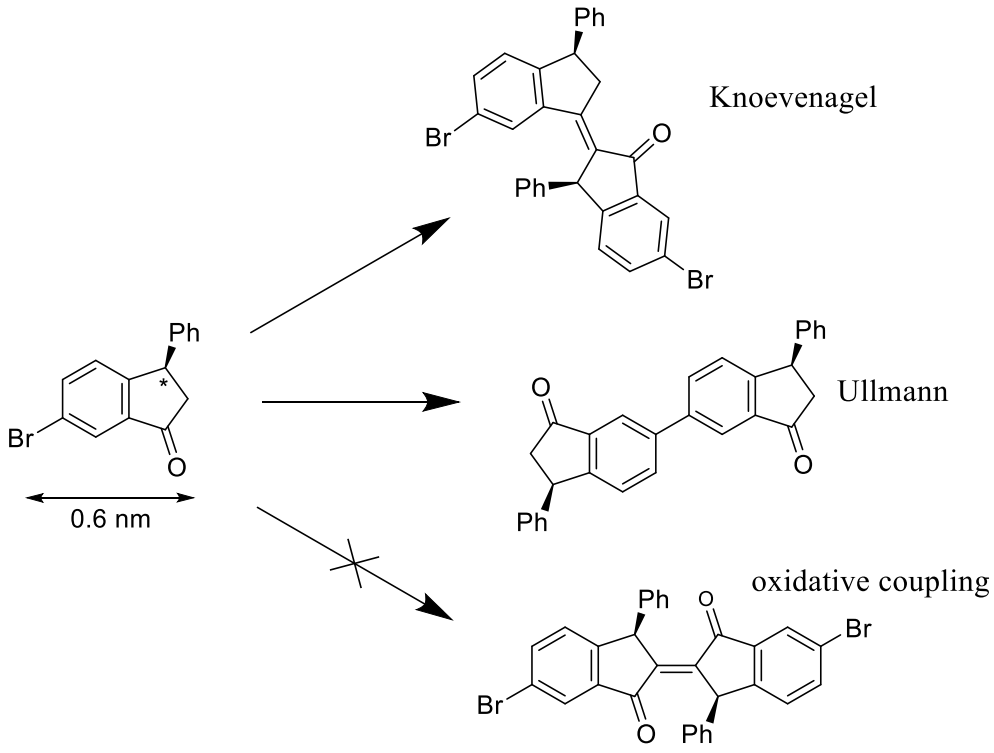

Figure 1: Molecular structure of (*R*)-6-bromo-3-phenyl-2,3-dihydro-1*H*-inden-1-one (BrPhINDO) and expected homocoupling reaction schemes. The oxidative coupling[29] was not observed on Cu(111).

Results and Discussion

Description of STM results

In a first part, we consider the *R*-stereoisomer of the chiral BrPhINDO precursor. The room-temperature deposition in submonolayer regime resulted in several different features rendering difficult to single out the intermolecular interactions possibly at play. A deposition close to one monolayer on the substrate kept at 100 °C was then performed, resulting in a much more homogeneous phase (Fig. 2a). Subsequently, annealing at increasing temperatures was performed to activate different intermolecular interactions (Fig. 2b-d). In the as-deposited sample, two main features were observed, both ascribable to supramolecular arrangements of a common building block. The most abundant motif consists of molecular chains (type-1 chains, pink rectangle in Fig. 2a) about 7-10 nm long and 2.6 nm wide in which the repeating units arrange in coupled parallel rows with an apparent periodicity of 0.25 nm along the rows. At the end of these rows or in between them, a less abundant structure, sometimes fused within, is present: a molecular ring made of three sub-units, presenting a C_3 symmetry (green circle in Fig. 2a), called α structure in the following. The building block in the chains and in the α structures is imaged as an oval feature of size 0.9 nm×0.7 nm, close to the indane backbone size of the BrPhINDO molecule. No contrast asymmetry is detected in each sub-unit (Fig. 3a), suggesting that the phenyl ring may have left the molecule or is not involved in the imaging contrast due to its out-of-plane orientation. A combination of metal-ligand coordination (or direct bonding to the metal surface atoms[38]) and hydrogen bonding can be envisaged as the driving force for the formation of these structures, especially considering the ability of such halogenated molecules to debrominate[39,40] that is also confirmed by the XPS analysis below. Nevertheless, the details of this non-covalent bonding are out of the scope of this study and will not be discussed further.

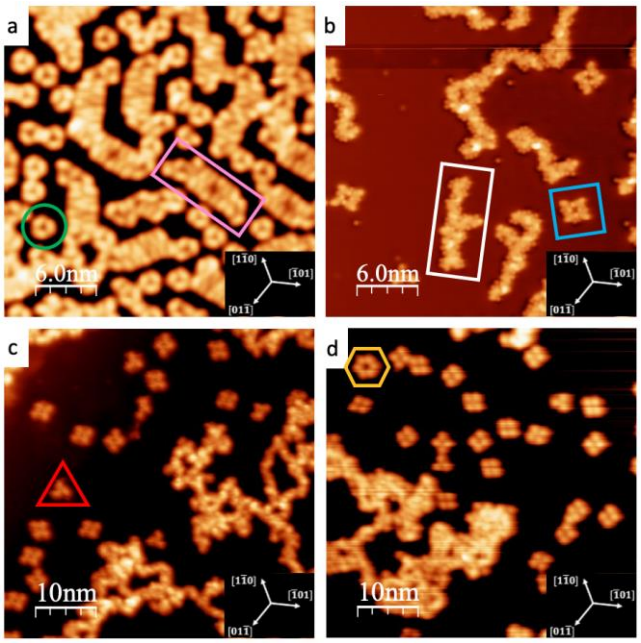

Figure 2: LT-STM images obtained after deposition of R-BrPhINDO molecule on hot Cu (111) surface (T_{Cu} = 100 °C) (a) and after annealing at 200 °C (b), 300 °C (c), and 400 °C (d). The different features are highlighted by colored frames: green circle for α structure, pink rectangle for type-1 chains, blue square for γ structure, white rectangle for type-2 chains, red triangle for β structure and yellow hexagon for δ structure.

Upon annealing at 200 °C, the coverage is reduced by more than 50 % due to substantial desorption. The precursor diffusion is then increased, facilitating intermolecular coupling and resulting in two main outcomes: elongated type-2 chains (white rectangle in Fig. 2b) and isolated well-defined γ structures displaying C_2 symmetry (highlighted by a blue square in Fig. 2b). By annealing at higher temperatures (Fig. 2c-d), the type-2 chains evolve in longer and intertwined structures whereas new isolated features appear sparsely next to the —now more abundant— γ forms: features with C_3 symmetry, named β (red triangle in Fig. 2c), and hexagonal features with C_3 symmetry (see below), named δ (yellow hexagon in Fig. 2d). Interestingly, all well-defined products obtained upon annealing above 100 °C display a defined chirality, as it will be discussed later. Concerning the type-2 chains, they are partially cross-linked and are about 8-24 nm long and 1-3 nm wide, in line with typical sizes for covalent polymerization of similar systems based on small aromatic precursors.[36,41-44] The presence of 1D extended chains testifies that both active sites designed for covalent coupling are activated at this temperature, together with possible co-operating metal-organic bonds. Nevertheless, due to their intricate and stochastic structure, the chain analysis does not allow a clear assignment of precursor evolution upon coupling. We then turn to the description of the isolated products γ, β and δ which, given their high temperature stability can be classified as covalent structures.

Model structures for the reaction products

Based on the LT-STM results and the expected reactivity of the precursor, we can suggest structural models for the products γ, β and δ. The precursor presents three sites likely to be activated on a surface, namely the Br, O and CH_2 sites able to promote the formation of covalent bonds through Ullmann, Knoevenagel and oxidative condensation reactions, respectively (see reaction schemes in Fig. 1). The STM images of the three covalent features and the corresponding structural models are presented in Fig. 3 (see also SI Fig. S2). Feature γ is composed of two "L"-shaped subunits. The best fit in size and shape for each of these subunits is realized by considering four monomers corresponding to two Ullmann-coupled dimers linked through a Knoevenagel reaction. The indanone moieties of the two subunits can then bind through hydrogen bonding in a head to tail fashion conferring a chiral C_2 symmetry character to the structure. The less abundant β structure is made up of smaller branches and is then not likely to derive from the γ feature. In fact, when low coverage samples are explored (not shown), the β feature is found already for annealing at 200 °C, thus enlarging its actual stability range. The best fit to the STM images of the β product is obtained by considering three Ullmann-coupled dimers, assembled by H-bonds and with a chiral C_3 symmetry. The β structures tend to disappear at higher annealing temperatures (see below), possibly by forming higher level products such as γ and δ. The feature δ appears at 300 °C and grows as a function of the annealing temperature, suggesting a progression in the reaction pathway. In fact, feature δ is composed of a closed macro-ring obtained through alternating Ullmann and Knovenagel couplings (Fig. 3h). The small stress induced by the symmetry mismatch between the precursor composed of a non-benzenoid ring and the hexagonal macroring geometry is probably overcome by the energy gain in the formation of this macrocyclic covalent structure. It is interesting to note that in all the above models, the inclusion of oxidative couplings that could have occurred through the CH_2 groups (see Fig. 1) did not give satisfactory agreements to the STM and can thus be ruled out from the processes leading to the observed products.

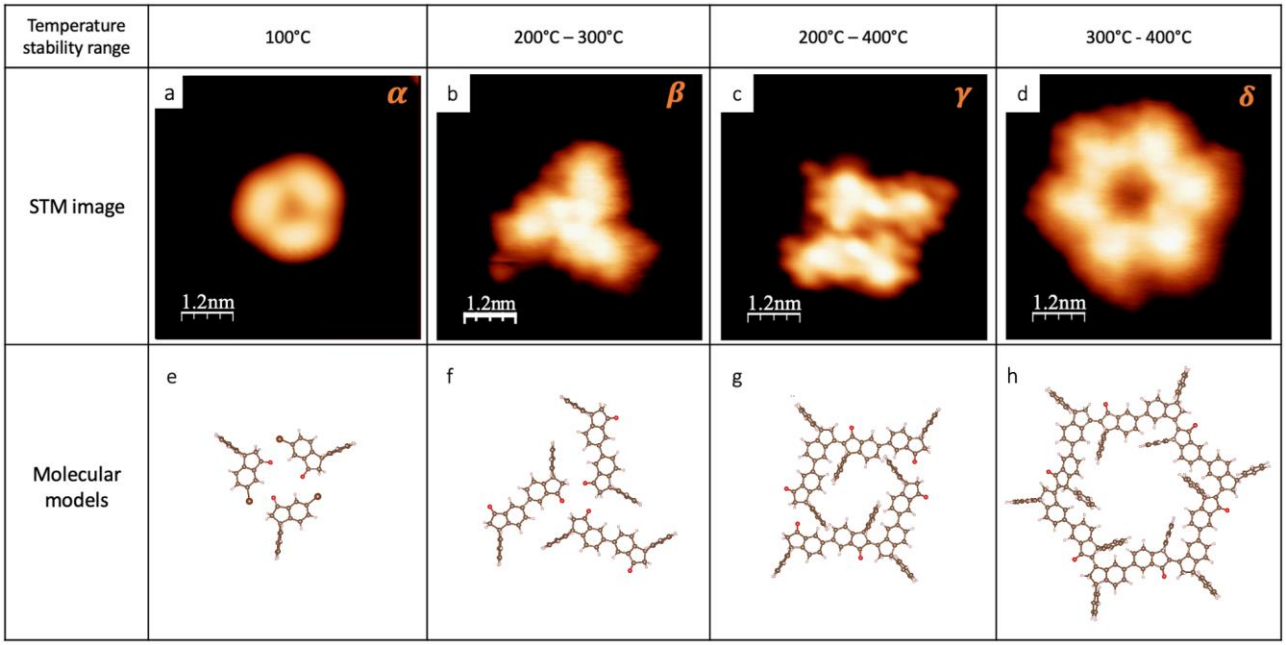

Figure 3: STM images and corresponding models of all observed isolated structures as a function of their stability range of temperature on the Cu(111) surface.

XPS measurements

As a support to the above models, additional XPS measurements were performed in a separate UHV system. The measurements being performed *ex-situ,* instead of trying to exactly reproduce the samples described above, we studied the evolution of a monolayer deposited at room temperature (RT) and sequentially annealed at increasing temperatures. Fig. 4 displays the XPS spectra of C 1s, O 1s and Br 3p core levels. All spectra display a single peak (or a spin-orbit doublet for Br 3p) with an asymmetric line shape, representative of multiple atomic sites. This may come either from the presence of different chemical environments within each molecule (as it is the case for the C 1s) or from different interactions with the substrate or between the molecules. In any case, given the inhomogeneous distribution of the different compounds in the present system, a deconvolution in multiple components to extract information about the molecular structures or intermolecular bonding is not relevant. The analysis will then focus on the main line binding energy (BE) position as well as the intensity ratios between the peaks.

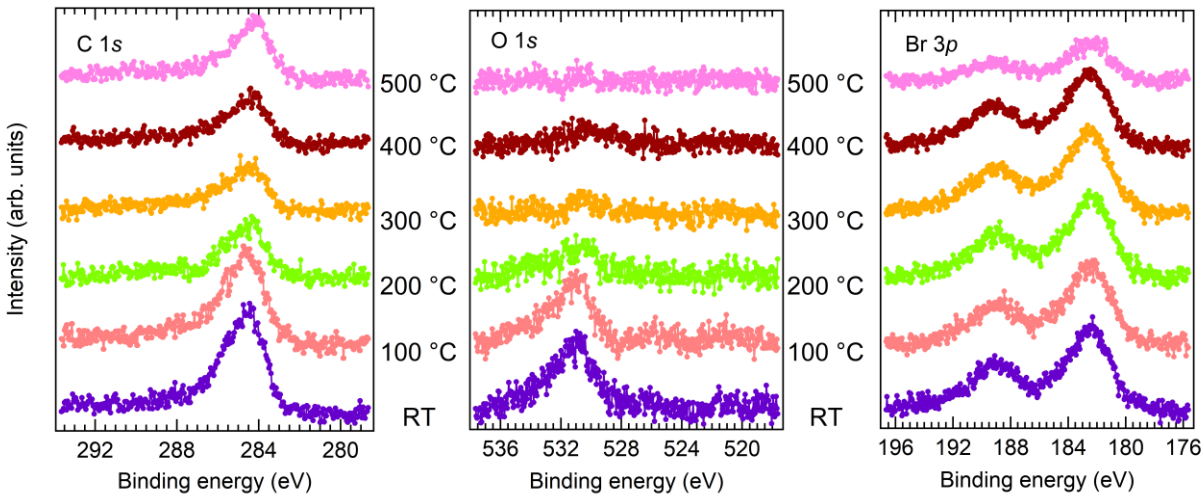

Figure 4: XPS data for BrPhINDO on Cu(111): C 1s (a), O 1s (b) and Br 3p (c) core levels as a function of the annealing temperature.

The Ullmann coupling reaction is very common when brominated precursors are adsorbed on coinage metal surfaces. In this reaction, as a first step, the debromination should occur and then, after a possible intermediate step in which C-metal adatom bonds are temporary formed, the as-created radical can induce C-C coupling. In the present XPS data, obtained at RT, the Br 3p spectrum is found at a BE of 182.5 eV, a value representative of Br adatoms on Cu surfaces.[45,46] Since the BE does not change as a function of temperature even when Br starts desorbing (above 500°C), one can conclude that the debromination occurs directly upon adsorption, as it is expected on Cu(111).[43,45] Unfortunately, the energy resolution does not allow to conclude on the presence of the C-Cu intermediate state which would manifest as a shoulder to the low BE side of the main C 1s peak.[39] With the aim of understanding the reactional mechanisms occurring on the surface, we computed the stoichiometric ratio between the carbon and the bromine atoms. Before the Ullmann and Knoevenagel covalent reactions set in, the stoichiometric ratio between the different chemical species composing the molecule should be reflected in the intensities of the respective core levels. For an intact BrPhINDO molecule, the expected C:Br ratio is 15 (see Fig. 1), while it should be 9 for a molecule having lost its phenyl functionalization since the desorption temperature of benzene lies below RT.[47] Upon adsorption at RT as well as after annealing at 100 °C the measured C:Br ratio is about 14, in line with a pristine precursor. As can be seen in Fig. 4, for 200 °C annealing temperature the C 1s intensity is sensibly reduced and the C:Br ratio decreased. Unfortunately, it is not possible to conclusively address this effect to a potential loss of phenyl functionalization. Indeed, while the Br adatoms remained adsorbed up to 500°C, part of this reduction can be attributed to the desorption of debrominated molecules, as also observed by STM. For higher annealing temperatures the C 1s peak

intensity stabilizes. This supports the picture in which the thermally activated reaction forms more stable compounds with no further loss of material upon annealing, in-line with the formation of covalently bonded superstructures. The thermal desorption should also affect the O 1s and indeed a net drop in peak intensity is observed at 200 °C. Here, the presence of substrate-related Auger peaks in this energy region makes the background subtraction difficult and prevents from a reliable measurement of the actual stoichiometry ratios of O with regard to C and Br. Interestingly, at variance with what is observed for C 1s, the O 1s exhibits a continuous decrease as the temperature increases. This behavior can be correlated with the progression of the Knoevenagel reaction with temperature, leading to the observed growth of the γ and δ populations and indicating that the Knoevenagel reaction is thermally activated as it has been already observed elsewhere.[24]

Prochirality of the reaction products

As observed above, all the isolated features resulting from the thermally activated covalent couplings of the *R*-BrPhINDO precursor show a defined prochirality on the surface. Prochirality is here defined as the loss of symmetry induced by the planar adsorption, i.e. on which side the molecule is lying on the surface. In BrPhINDO, the phenyl function is bonded to a carbon atom with sp^3 hybridization. Its out-of-plane configuration with respect to the indanone backbone is meant to guide the prochiral adsorption configuration of the molecule and, in turn, to determine the prochiral character of the reaction products. In the model structures of Fig. 3, the indanone plane is lying flat on the surface and the phenyl group is pointing outwards, thus providing a defined prochiral symmetry of the structures in agreement with the STM images shown here. In fact, we also observed a substantial number of structures presenting the opposite prochirality, with an abundance of 15 to 30 % (see Fig. 5).

To account for such prochirality inversion, two distinct mechanisms can be proposed (see SI Fig. S3). A loss of the phenyl group upon adsorption would remove the intrinsic chirality of the precursor and the two prochiral adsorption configurations can be achieved by flipping of the adsorption side. On the other hand, a chiral inversion of the asymmetric carbon could occur leading to an inversion of the more favorable adsorption side of the indanone moiety. Similar internal modifications of the precursor such as spontaneous conformational changes were previously reported.[30,31,48,49] Whichever the origin of the prochirality inversion, the larger abundance of the original chirality in the reaction products suggests a relatively high energy barrier for the process. XPS data indicate that, at RT and after annealing at 100 °C, there is no degradation of the molecule other than the Br loss, thus indicating that the phenyl functions are still attached to the molecules deposited at that temperature. In any case, the enantiomeric asymmetry is preserved even at high annealing temperature, so the

racemization process is not further evolving. The chiral inversion is thus taking place at lower temperature, most probably when the precursors are not covalently linked.

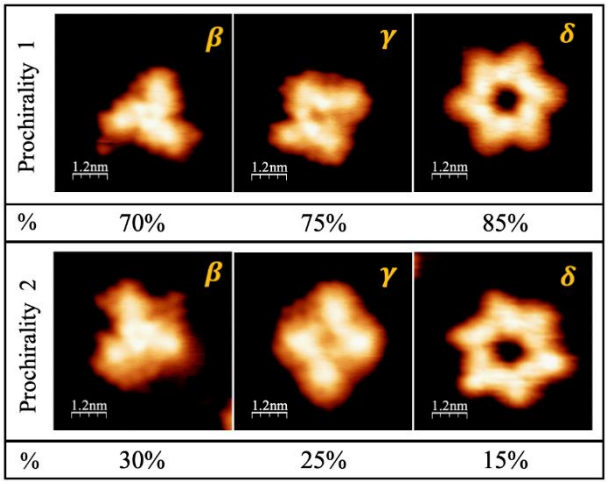

Figure 5: STM images showing the two prochiralities and their relative abundance observed for the β, γ and δ-structures obtained after deposition of the molecule *R*-BrPhINDO on Cu(111).

In order to verify this chiral asymmetry, the other enantiomer of the same molecule (*S*-BrPhINDO) was deposited on the Cu(111) surface and studied in similar conditions (see S.I. Fig. S4 and Table S1). In this case also, the two prochirality forms of all the structures (β, γ, δ) are observed. As expected, the distribution of these two prochirality forms on the surface is reversed, thus confirming the partial racemic inversion that is taking place on the Cu(111) surface.

Conclusions

In summary, by employing a new precursor with multiple reaction sites, namely (*R*)-6-bromo-3-phenyl-2,3-dihydro-1*H*-inden-1-one (BrPhINDO), different reaction products were synthesized on Cu(111) as a function of the annealing temperature. H-bonded C_3 threefold assemblies of Ullmann-coupled dimers were singled out as the smallest reacted entities. Knoevenagel reactions between these dimers resulted in the formation of tetramers coupled twofold to form larger C_2 structures. Finally, three tetramers further couple through Knoevenagel reactions to produce large C_3 hexagons. All structures present a defined prochirality with an asymmetric enantiomeric distribution due to the occurrence of chiral inversion for a fraction of the precursors (partial racemization). The latter is imputed to a phenyl loss or to a chiral switch upon adsorption.

Experimental section

Chemical synthesis of (*R*)-6-bromo-3-phenyl-2,3-dihydro-1*H*-inden-1-one (BrPhINDO)

See also Supporting Information for additional details.

- Synthesis of 6-bromo-1*H*-inden-1-one:

N-bromosuccinimide (NBS) (2.7 g, 1.1 eq.) and azobisisobutyronitrile (AIBN) (30 mg, 0.01 eq.) were added to a 1,2-dichloroethane solution (60 mL) of 6-bromo-2,3-dihydro-1*H*-inden-1-one (3 g, 1 eq., 14.2 mmol). The resulting mixture was stirred at reflux temperature for 2.5 h, then cooled and filtered through Celite, washed with CH_2Cl_2 and evaporated. The filtrate was cooled to 0 °C and treated with triethylamine (0.6 mL, 6.0 mmol) overnight, then concentrated in vacuo. The crude product was chromatographed (1 : 9~1 : 4 EtOAc/pentane, flash with acetone) and afforded the 6-bromo-1*H*-inden-1-one as a brown solid (m = 1.2 g, 45% yield).

^{1}H NMR (300 MHz, $CDCl_3$) δ: 7.55 (dd, *J* = 6.0, 0.9 Hz, 1H), 7.41 (dd, *J* = 7.6, 1.6 Hz, 1H), 7.30 (d, *J* = 7.6 Hz, 1H), 7.23 (d, *J* = 1.6 Hz, 1H), 5.95 (d, *J* = 6.0 Hz, 1H).

- Synthesis of 6-bromo-3-phenyl-2,3-dihydro-1*H*-inden-1-one (BrPhINDO):

A solution composed of copper iodide (3.1 g, 2.7 eq.), sodium iodide (4.5 g, 5 eq.), dimethylsulfide (3.6 mL, 8 eq.) in DCM (50 mL) was cooled to -78°C. Then, phenyl lithium (7.92 mL, 1.9 M in dibuthylether, 2.5 eq.) was added followed by chlorotrimethylsilane (0.63 mL, 5 eq.) and the solution was stirred at -78°C for 20 min. Then, the 6-bromo-1H-inden-1-one (1.2 g, 6 mmol, 1eq.), dissolved in DCM (50 mL), was added and the reaction mixture was allowed to warm to 0°C. The solution was stirred at this temperature for 9 hours and finally at room temperature. The mixture was quenched with half saturated ammonium chloride (20 mL) and then filtered. Afterwards, the crude was extracted with DCM (3 x 25 mL), washed with sodium thiosulfate, dried over magnesium sulfate and the solvent removed under reduced pressure. The residue was purified by column chromatography (SiO_2) using DCM as the eluent. The product was isolated as a yellow oil (1.3 g, 4.7 mmol, 78 % yield).

^{1}H NMR (300 MHz, $CDCl_3$) δ: 7.93 (s, 1H), 7.66 (dd, *J* = 8.2, 1.8 Hz, 1H), 7.31 (dd, *J* = 13.4, 5.9 Hz, 3H), 7.13 (dd, *J* = 15.2, 7.6 Hz, 3H), 4.52 (dd, *J* = 7.9, 3.8 Hz, 1H), 3.25 (dd, *J* = 19.4, 8.1 Hz, 1H), 2.71 (dd, *J* = 19.4, 3.8 Hz, 1H).

- Fits with literature data: Ref. [50]
- Semi-preparative Chiral HPLC

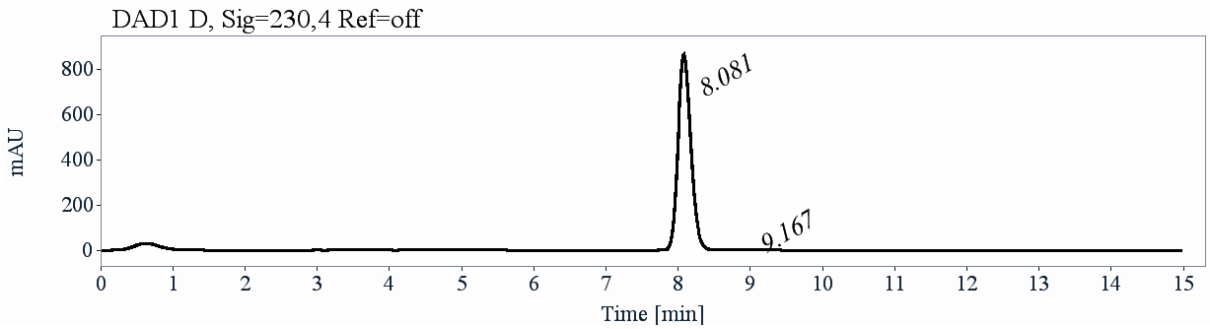

- Sample preparation: About 175 mg of compound 4-Br-INDO-Ph are dissolved in 7 mL of a mixture of hexane / isopropanol / ethanol / dichloromethane (46/12/28/14).
- Chromatographic conditions: Chiralpak IG (250 x 10 mm), hexane/isopropanol (80/20) as mobile phase, flow-rate = 5 mL/min, UV detection at 254 nm.
- Injections (stacked): 70 times 100 mL, every 9.4 minutes.

Scanning Tunneling Microscopy

The experiments were performed in an ultrahigh vacuum UHV setup (base pressure ~10^{-10} mbar) consisting of a preparation chamber for sample cleaning and molecular deposition and an analysis chamber for low-temperature scanning tunneling microscopy (Scienta Omicron Infinity LT-STM, T=9 K). The Cu(111) surface was prepared by several cycles of sputtering Ar^+ (1.0 KeV) and annealing to 550°C to obtain an atomically clean surface with large terraces. The BrPhINDO molecules were evaporated from a crucible heated at 30°C and deposited on the Cu(111) surface held at a fixed temperature (RT or 100°C). STM experiments were acquired in constant-current mode with the voltage applied to the sample (typical values I=50 to 500 pA, V= -1.3 to +1.3 V) with a Nanonis RC5 electronic controller. Images were analyzed with the WSxM software.[51]

XPS experiments

X-ray photoelectron spectroscopy (XPS) was carried out with a non-monochromatized Al K α line (h ν = 1486.6 eV) of an X-ray tube from PREVAC. The emitted photoelectrons were counted using a R3000 analyzer from ScientaOmicron, equipped with a micro-channel plate detector. The resolution in XPS measurements, determined from the full width at half-maximum of Cu 3d core levels recorded on the clean surface, was 0.9 eV. All spectra are background subtracted and referenced to the substrate Fermi level.

Acknowledgements

We thank Nataliya Kalashnyk for motivating this research topic. Laurent Nony, Christian Loppacher and Franck Para are gratefully acknowledged for experimental support. The project leading to this publication has received funding from Agence Nationale de la Recherche (ANR Grant N° ANR-17-CE08-0010 “DUALITY”).

References

(1) Sweetman, A.; Champness, N. R.; Saywell, A. On-surface chemical reactions characterised by ultra-high resolution scanning probe microscopy. *Chem. Soc. Rev.* **2020,** *49*, 4189-4202.
(2) Grill, L.; Hecht, S. Covalent on-surface polymerization. *Nat. Chem.* **2020,** *12*, 115-130.
(3) Palmino, F.; Loppacher, C.; Cherioux, F. Photochemistry Highlights on On-Surface Synthesis. *ChemPhysChem* **2019,** *20*, 2271-2280.
(4) Clair, S.; De Oteyza, D. G. Controlling a Chemical Coupling Reaction on a Surface: Tools and Strategies for On-Surface Synthesis. *Chem. Rev.* **2019,** *119*, 4717-4776.
(5) Held, P. A.; Fuchs, H.; Studer, A. Covalent-Bond Formation via On-Surface Chemistry. *Chem. Eur. J.* **2017,** *23*, 5874-5892.
(6) Lackinger, M. On-Surface Polymerization - a Versatile Synthetic Route to Two-Dimensional Polymers. *Polym. Int.* **2015,** *64*, 1073-1078.
(7) Mendez, J.; Lopez, M. F.; Martin-Gago, J. A. On-surface synthesis of cyclic organic molecules. *Chem. Soc. Rev.* **2011,** *40*, 4578–4590.
(8) Fan, Q.; Gottfried, J. M.; Zhu, J. Surface-Catalyzed C–C Covalent Coupling Strategies toward the Synthesis of Low-Dimensional Carbon-Based Nanostructures. *Acc. Chem. Res.* **2015,** *48*, 2484–2494.
(9) Hla, S.-W.; Bartels, L.; Meyer, G.; Rieder, K.-H. Inducing All Steps of a Chemical Reaction with the Scanning Tunneling Microscope Tip : Towards Single Molecule Engineering. *Phys. Rev. Lett.* **2000,** *85*, 2777-2780.
(10) Grill, L.; Dyer, M.; Lafferentz, L.; Persson, M.; Peters, M. V.; Hecht, S. Nano-Architectures by Covalent Assembly of Molecular Building Blocks. *Nat. Nanotechnol.* **2007,** *2*, 687-691.
(11) Cai, J. M.; Ruffieux, P.; Jaafar, R.; Bieri, M.; Braun, T.; Blankenburg, S.; Muoth, M.; Seitsonen, A. P.; Saleh, M.; Feng, X.; et al. Atomically Precise Bottom-Up Fabrication of Graphene Nanoribbons. *Nature* **2010,** *466*, 470-473.
(12) Lafferentz, L.; Eberhardt, V.; Dri, C.; Africh, C.; Comelli, G.; Esch, F.; Hecht, S.; Grill, L. Controlling On-Surface Polymerization by Hierarchical and Substrate-Directed Growth. *Nat. Chem.* **2012,** *4*, 215-220.
(13) Peyrot, D.; Silly, M. G.; Silly, F. Temperature-Triggered Sequential On-Surface Synthesis of One and Two Covalently Bonded Porous Organic Nanoarchitectures on Au(111). *J. Phys. Chem. C* **2017,** *121*, 26815-26821.
(14) Galeotti, G.; De Marchi, F.; Hamzehpoor, E.; MacLean, O.; Rao, M. R.; Chen, Y.; Besteiro, L. V.; Dettmann, D.; Ferrari, L.; Frezza, F.; et al. Synthesis of mesoscale ordered two-dimensional pi-conjugated polymers with semiconducting properties. *Nat. Mater.* **2020,** *19*, 874-880.

(15) Grossmann, L.; King, B. T.; Reichlmaier, S.; Hartmann, N.; Rosen, J.; Heckl, W. M.; Bjork, J.; Lackinger, M. On-surface photopolymerization of two-dimensional polymers ordered on the mesoscale. *Nat. Chem.* **2021,** *13*, 730.
(16) Lipton-Duffin, J. A.; Ivasenko, O.; Perepichka, D. F.; Rosei, F. Synthesis of Polyphenylene Molecular Wires by Surface-Confined Polymerization. *Small* **2009,** *5*, 592-597.
(17) Bieri, M.; Treier, M.; Cai, J. M.; Ait-Mansour, K.; Ruffieux, P.; Gröning, O.; Gröning, P.; Kastler, M.; Rieger, R.; Feng, X. L.; et al. Porous Graphenes: Two-Dimensional Polymer Synthesis with Atomic Precision. *Chem. Commun.* **2009,** *45*, 6919-6921.
(18) Lackinger, M. Surface-Assisted Ullmann Coupling. *Chem. Commun.* **2017,** *53*, 7872-7885.
(19) Zhang, Y. Q.; Kepcija, N.; Kleinschrodt, M.; Diller, K.; Fischer, S.; Papageorgiou, A. C.; Allegretti, F.; Bjork, J.; Klyatskaya, S.; Klappenberger, F.; et al. Homo-Coupling of Terminal Alkynes on a Noble Metal Surface. *Nat. Commun.* **2012,** *3*, 1286.
(20) Gao, H. Y.; Wagner, H.; Zhong, D. Y.; Franke, J. H.; Studer, A.; Fuchs, H. Glaser Coupling at Metal Surfaces. *Angew. Chem. Int. Ed.* **2013,** *52*, 4024-4028.
(21) Saywell, A.; Browning, A. S.; Rahe, P.; Anderson, H. L.; Beton, P. H. Organisation and ordering of 1D porphyrin polymers synthesised by on-surface Glaser coupling. *Chem. Commun.* **2016,** *52*, 10342-10345.
(22) Au-Yeung, K. H.; Kuhne, T.; Becker, D.; Richter, M.; Ryndyk, D. A.; Cuniberti, G.; Heine, T.; Feng, X. L.; Moresco, F. On-Surface Formation of Cyano-Vinylene Linked Chains by Knoevenagel Condensation. *Chem. Eur. J.* **2021,** *27*, 17336-17340.
(23) Geng, Y. F.; Dai, H. L.; Chang, S. Q.; Hu, F. Y.; Zeng, Q. D.; Wang, C. Formation of C=C Bond via Knoevenagel Reaction between Aromatic Aldehyde and Barbituric Acid at Liquid/HOPG and Vapor/HOPG Interfaces. *ACS Appl. Mater. Interfaces* **2015,** *7*, 4659-4666.
(24) Kalashnyk, N.; Salomon, E.; Mun, S. H.; Jung, J.; Giovanelli, L.; Angot, T.; Dumur, F.; Gigmes, D.; Clair, S. The Orientation of Silver Surfaces Drives the Reactivity and the Selectivity in Homo-Coupling Reactions. *ChemPhysChem* **2018,** *19*, 1802-1808.
(25) Krief, P.; Becker, J. Y.; Ellern, A.; Khodorkovsky, V.; Neilands, O.; Shapiro, L. s-indacene-1,3,5,7(2H,6H)-tetraone ('Janus dione') and 1,3-dioxo-5,6-indane-dicarboxylic acid: Old and new 1,3-indandione derivatives. *Synthesis-Stuttgart* **2004,** *15*, 2509-2512.
(26) Sprick, R. S.; Thomas, A.; Scherf, U. Acid catalyzed synthesis of carbonyl-functionalized microporous ladder polymers with high surface area. *Polymer Chemistry* **2010,** *1*, 283-285.
(27) Kalashnyk, N.; Clair, S. Self-Accommodating Honeycomb Networks from Supramolecular Self-Assembly of s-Indacene-tetrone on Silver Surfaces. *Langmuir* **2022,** *38*, 1067-1071.
(28) Kalashnyk, N.; Dumur, F.; Gigmes, D.; Clair, S. Molecular adaptation in supramolecular self-assembly: brickwall-type phases of indacene-tetrone on silver surfaces. *Chem. Commun.* **2018,** *54*, 8510-8513.
(29) Kalashnyk, N.; Mouhat, K.; Oh, J.; Jung, J.; Xie, Y.; Salomon, E.; Angot, T.; Dumur, F.; Gigmes, D.; Clair, S. On-Surface Synthesis of Aligned Functional Nanoribbons Monitored by Scanning Tunneling Microscopy and Vibrational Spectroscopy. *Nat. Commun.* **2017,** *8*, 14735.
(30) Nuermaimaiti, A.; Bombis, C.; Knudsen, M. M.; Cramer, J. R.; Laegsgaard, E.; Besenbacher, F.; Gothelf, K. V.; Linderoth, T. R. Chiral Induction with Chiral Conformational Switches in the Limit of Low "Sergeants to Soldiers" Ratio. *ACS Nano* **2014,** *8*, 8074-8081.
(31) Weigelt, S.; Busse, C.; Petersen, L.; Rauls, E.; Hammer, B.; Gothelf, K. V.; Besenbacher, F.; Linderoth, T. R. Chiral switching by spontaneous conformational change in adsorbed organic molecules. *Nat. Mater.* **2006,** *5*, 112-117.
(32) Xu, Y.; Duan, J. J.; Yi, Z. Y.; Zhang, K. X.; Chen, T.; Wang, D. Chirality of molecular nanostructures on surfaces via molecular assembly and reaction: manifestation and control. *Surf. Sci. Rep.* **2021,** *76*, 100531.

(33) Zaera, F. Chirality in adsorption on solid surfaces. *Chem. Soc. Rev.* **2017,** *46*, 7374-7398.
(34) Faury, T.; Clair, S.; Abel, M.; Dumur, F.; Gigmes, D.; Porte, L. Sequential Linking to Control the Growth of a Surface Covalent Organic Framework. *J. Phys. Chem. C* **2012,** *116*, 4819-4823.
(35) Pigot, C.; Dumur, F. Recent Advances of Hierarchical and Sequential Growth of Macromolecular Organic Structures on Surface. *Materials* **2019,** *12*, 662.
(36) Giovanelli, L.; Pawlak, R.; Hussein, F.; Maclean, O.; Rosei, F.; Song, W.; Pigot, C.; Dumur, F.; Gigmes, D.; Ksari, Y.; et al. On-surface synthesis of unsaturated hydrocarbon chains through C-S activation. *Chem. Eur. J.* **2022,** *28*, e202200809.
(37) Dong, L.; Liu, P. N.; Lin, N. Surface-Activated Coupling Reactions Confined on a Surface. *Acc. Chem. Res.* **2015,** *48*, 2765-2774.
(38) Bieri, M.; Nguyen, M. T.; Gröning, O.; Cai, J. M.; Treier, M.; Ait-Mansour, K.; Ruffieux, P.; Pignedoli, C. A.; Passerone, D.; Kastler, M.; et al. Two-Dimensional Polymer Formation on Surfaces: Insight into the Roles of Precursor Mobility and Reactivity. *J. Am. Chem. Soc.* **2010,** *132*, 16669-16676.
(39) Di Giovannantonio, M.; El Garah, M.; Lipton-Duffin, J.; Meunier, V.; Cardenas, L.; Fagot-Revurat, Y.; Cossaro, A.; Verdini, A.; Perepichka, D. F.; Rosei, F.; et al. Insight into Organometallic Intermediate and Its Evolution to Covalent Bonding in Surface-Confined Ullmann Polymerization. *ACS Nano* **2013,** *7*, 8190-8198.
(40) Björk, J.; Hanke, F.; Stafstrom, S. Mechanisms of Halogen-Based Covalent Self-Assembly on Metal Surfaces. *J. Am. Chem. Soc.* **2013,** *135*, 5768-5775.
(41) Sedona, F.; Fakhrabadi, M. M. S.; Carlotto, S.; Mohebbi, E.; De Boni, F.; Casalini, S.; Casarin, M.; Sambi, M. On-surface synthesis of extended linear graphyne molecular wires by protecting the alkynyl group. *Phys. Chem. Chem. Phys.* **2020,** *22*, 12180-12186.
(42) Smerieri, M.; Pis, I.; Ferrighi, L.; Nappini, S.; Lusuan, A.; Vattuone, L.; Vaghi, L.; Papagni, A.; Magnano, E.; Di Valentin, C.; et al. Synthesis of Corrugated C-Based Nanostructures by Br-Corannulene Oligomerization. *Phys. Chem. Chem. Phys.* **2018,** *20*, 26161-26172.
(43) Galeotti, G.; De Marchi, F.; Taerum, T.; Besteiro, L. V.; El Garah, M.; Lipton-Duffin, J.; Ebrahimi, M.; Perepichka, D. F.; Rosei, F. Surface-Mediated Assembly, Polymerization and Degradation of Thiophene-Based Monomers. *Chem. Sci.* **2019,** *10*, 5167-5175.
(44) Deimel, P. S.; Stoiber, K.; Jiang, L.; Lloyd, J. A.; Oh, S. C.; Fischer, S.; Saglam, O.; Schlichting, H.; Papageorgiou, A. C.; Barth, J. V.; et al. Bisphenol A and Diethylstilbestrol on Cu(111): On-Surface Polymerization Initiated by Hydroxy-Directed Ortho C-H Bond Activation. *J. Phys. Chem. C* **2019,** *123*, 1354-1361.
(45) Chen, M.; Xiao, J.; Steinruck, H. P.; Wang, S. Y.; Wang, W. H.; Lin, N.; Hieringer, W.; Gottfried, J. M. Combined Photoemission and Scanning Tunneling Microscopy Study of the Surface-Assisted Ullmann Coupling Reaction. *J. Phys. Chem. C* **2014,** *118*, 6820-6830.
(46) Abyazisani, M.; MacLeod, J. M.; Lipton-Duffin, J. Cleaning up after the Party: Removing the Byproducts of On-Surface Ullmann Coupling. *ACS Nano* **2019,** *13*, 9270-9278.
(47) Lukas, S.; Vollmer, S.; Witte, G.; Woll, C. Adsorption of acenes on flat and vicinal Cu(111) surfaces: Step induced formation of lateral order. *J. Chem. Phys.* **2001,** *114*, 10123-10130.
(48) Goubert, G.; Dong, Y.; Groves, M. N.; Lemay, J. C.; Hammer, B.; McBreen, P. H. Monitoring interconversion between stereochemical states in single chirality-transfer complexes on a platinum surface. *Nat. Chem.* **2017,** *9*, 531-536.
(49) Ammon, M.; Sander, T.; Maier, S. On-Surface Synthesis of Porous Carbon Nanoribbons from Polymer Chains. *J. Am. Chem. Soc.* **2017,** *139*, 12976-12984.
(50) Parveen, N.; Sekar, G. Palladium Nanoparticles-Catalyzed Synthesis of Indanone Derivatives via Intramolecular Reductive Heck Reaction. *Adv. Synth. Catal.* **2019,** *361*, 4581-4595.

(51) Horcas, I.; Fernández, R.; Gómez-Rodríguez, J. M.; Colchero, J.; Gómez-Herrero, J.; Baro, A. M. WSXM: A software for scanning probe microscopy and a tool for nanotechnology. *Rev. Sci. Inst.* **2007,** *78*, 013705.